Scouting Novel Protein Kinase A (PKA) Inhibitors by Using a Consensus Docking-Based Virtual Screening Approach

Nicola Zonta[1], Giorgio Cozza[2], Alessandra Gianoncelli[2], Oliver Korb[3], Thomas E. Exner[3], Flavio Meggio[2], Giuseppe Zagotto[1] and Stefano Moro*,[1]

[1]*Molecular Modeling Section (MMS), Dipartimento di Scienze Farmaceutiche, Università di Padova, via Marzolo 5, Padova, Italy*

[2]*Dipartimento di Chimica Biologica, Viale G. Colombo 3, Università di Padova, 35121 Padova, Italy*

[3]*Theoretische Chemische Dynamik, Universität Konstanz, Konstanz, Germany*

Abstract: Virtual screening (VS) approaches have been constantly increasing their applications into hit discovery process.

In the last few years, we have performed an intensive screening campaign using different *in silico* strategies and combining them with a biochemistry validation. In the present work, using a consensus docking approach, we have identified a small family of novel protein kinase A (PKA) inhibitors. In particular, an anthraquinone derivative (compound **11**) has shown an interesting inhibitory activity versus PKA with an IC_{50} value of 27 μM.

Keywords: Virtual screening (VS), Molecular docking, Protein kinase A (PKA).

INTRODUCTION

Discovering new drug candidates through virtual screening (VS) of large chemical databases targeting protein structures has shown great promise [1]. With the dramatic increase of pharmaceutical targets in recent years arising from the human genome project and high-throughput crystallography efforts, virtual screening will undoubtedly play a crucial role in identifying novel ligands for the new coming therapeutically relevant protein targets [1].

There are two fundamental approaches to virtually screen molecular databases: a ligand-based (pharmacophore-driven) virtual screening, and a structure-based (3D target-driven) virtual screening. The power of pharmacophore-driven methods for lead generation lies in their ability to suggest a diverse set of compounds potentially possessing a desired biological activity but which has totally different chemical scaffolds. Structure-based VS searches a database for compounds that fit into the binding site of the target, based on their chemical feature matching and shape complementarity. However, structure-based studies require 3D knowledge of the target. Molecular docking represents the heart of a structure-based VS procedure. It has to solve two distinct, but highly correlated problems: the prediction of the most favorable inhibitor conformation (pose) inside the target structure's active pocket and the prediction of its corresponding binding affinity. The two faces of the same coin are the exhaustive exploration of the ligand conformational space inside the protein cleft and the estimation of the different energy contributions to the free energy of binding [2].

Nowadays, several virtual screening protocols have been proposed. For docking programs, the primary criteria to assess their performance are docking accuracy (RMSD to known pose), scoring accuracy (prediction of the absolute binding free energy), screening efficiency (discrimination of active hits from random compounds), and computational speed (time needed to perform the conformational sampling). Computational speed that is strongly dependent on the docking algorithm used is vital in virtual screening. Only those able to dock a flexible ligand within a reasonable time scale (100–200s) are suitable for virtual screening purpose [3-7]. Unfortunately, none of the present methods is able to satisfactorily fulfill all these requirements, i.e. to offer a robust, accurate, and fast solution to the docking problem.

In the last few years, we have performed an intensive screening campaign using different *in silico* strategies and combining them with a biochemistry validation [8,9]. In the presented paper, we have focused our attention on protein kinase A (PKA) due to its key role in cancer [10]. Following some recent successful examples of new kinase inhibitors discovered by high-throughput docking (HTD) [8], we have performed a virtual screening experiment targeting the ATP binding site of PKA by browsing our in house molecular database (MMsINC) [11].

MATERIAL AND METHODS

Generally speaking, HTD approach could represent a good strategy to prioritize compounds for chemical synthesis and biological screening. In our virtual screening protocol, we have used a combination of different HTD protocols in tandem with a consensus scoring strategy, as summarized in Fig. (**1**). Each step will be described in more detail in the following sections.

Preparation of Protein Structures

Nine different PKA structures in complex with different ligands were obtained from the Protein Data Bank [12] (PDB

*Address correspondence to this author at the Molecular Modeling Section (MMS), Department of Pharmaceutical Sciences, University of Padova, Via Marzolo, 5 – 35131 Padova, Italy; Tel: +39 049 8275704; Fax: +39 049 827 5366; E-mail: stefano.moro@unipd.it

Fig. (1). Flowchart of the high-throughput consensus docking.

codes are summarized in Table **1**). Water molecules, ions and the ligands were removed and only the main PKA catalytic domain chain was kept. Hydrogen atoms were added reflecting the protonation state at physiological pH using MOE suite [13], and the resulting structures were carefully checked for missing connectivity or inconsistent protonation states.

Protein structures were energy-minimized in MOE using Amber 99 force field and freezing the coordinates all protein heavy atoms.

Preparation of PKA Inhibitors and Molecular Database (MMsINC)

Ligand structures were energy-minimized using the MMFF94x force field in MOE, and then refined with the LigPrep [14] utility available in Maestro (Schrödinger Inc.), predicting the most probable tautomeric and ionic forms of each ligand structure at pH= 7.

Consensus Scoring Functions

Consensus scoring methods have been previously reported to be an alternative and valid approach to balance the contributions of different scoring functions, thus, improving their overall performance [15, 16]. In this approach, we investigated the performance of three different consensus scoring functions.

a) *NCS*: a classical rank-by-rank approach. The score of this function for a given molecule is obtained by averaging the ranks r_i, it obtains from all the scoring functions.

$$NCS(x) = \frac{\sum_{i=1}^{n} r_i(x) - 1}{n}$$

b) *LCS*: a rank-by-score function. The score is calculated by averaging the contribution of each scoring func-

Table 1. PDB Entries Used in the Docking Validation

PDB Code	Resolution (Å)	Co-Crystallized Ligand
1RE8	2.1	1
1STC	2.3	2
1Q8T	2.0	3
1Q8U	1.9	4
1Q8W	2.2	5
1SZM	2.5	6
1YDR	2.2	7
1YDS	2.2	8
1YDT	2.3	9

tion's score $S_i(x)$ after normalizing to the same interval [0, 1]. The score is then multiplied by the number of entries in the database N minus one for direct comparison with NCS results.

$$LCS(x) = \frac{\sum_{i=1}^{n} \frac{M_i - S_i(x)}{M_i - m_i}}{n} \cdot (N-1)$$

Where M_i and m_i are the best and worst scoring function values of scoring function i for the database, respectively.

c) *FiTk:* This function represents the number of scoring functions, for which a certain molecule is scored among the top k% of the database.

$$FiTk(x) = \sum_{i=1}^{n} f(x)$$

$$f(x) = \begin{cases} 1 \text{ if } \frac{r_i - 1}{N-1} \in [0, \frac{k}{100}] \\ 0 \text{ if } \frac{r_i - 1}{N-1} \in]\frac{k}{100}, 1] \end{cases}$$

Scoring Functions

In the present work, a collection of 8 empirical scoring functions has been selected. Six of them are implemented in FRED docking suite [17], such as Chemgauss and Chemgauss2, Screenscore, Zapbind, Chemscore [18], and PLP [19]. Moreover, MOE-score [13] and X-Score [20] have also been also utilized as originally implemented in each docking program [21, 22].

Docking Algorithms

GOLD

GOLD [23], is among the most widely-used docking protocol. It implements a genetic algorithm in which the population is separated in groups ("islands"). Each island evolves independently of the others. A migration operator allows an individual to move from island to island with a certain probability. Standard parameter settings have been used.

PLANTS

The protein-ligand docking algorithm PLANTS [24, 25] is based on a class of stochastic search algorithms called Ant Colony Optimization (ACO). An artificial ant colony is employed to search for high quality protein-ligand conformations with respect to the given scoring function by mimicking the pheromone trail laying behavior of real ant colonies searching for food. PLANTS use an empirical scoring function called CHEMPLP. The default values of 20 ants, 0.25 pheromone evaporation factor and 1.0 sigma scaling factors were used as proposed in Korb *et al.* [24, 25].

MOE-Dock

We used the genetic docking algorithm implemented in MOE-Dock protocol of MOE suite [13]. Standard parameters settings have been used in each docking run.

GLIDE

Glide implements a systematic algorithm based on a hierarchical series of filters [26]. Conformations that successfully go through the last filter are energy-minimized and returned as solutions. We used the XP (extra precision) setting since its performance appeared to be significantly higher than the others (data not shown).

eHiTS

The search algorithm in *eHiTS* [27] is based on a divide and conquer approach. Each rigid fragment of a molecule is separately docked, and then a solution is build from high-score fragment poses. Different protonation states of ligand and protein are tested. Standard parameters have been used in each docking run.

Chemistry

The nitro-anthraquinone derivative (**15**) [28] was obtained by mild nitration of the corresponding 1,8-hydroxyl-

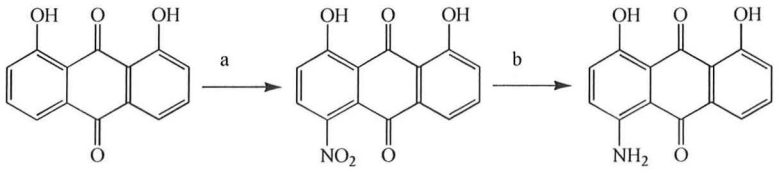

15 **10**

Scheme 1. a) CH_3COOH, KNO_3, 50°c for 15', then rt overnight; **b)** H_2, Pd/C, CH_3OH, rt, 4h.

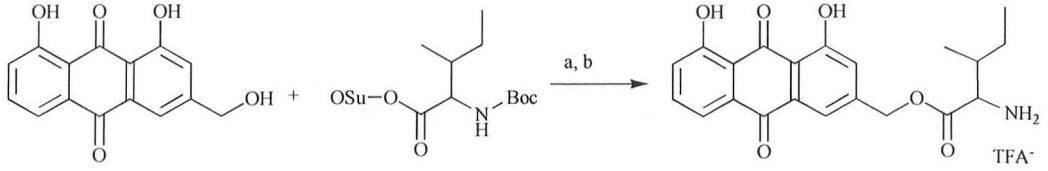

16 **11**

Scheme 2. a) Et_3N, DMAP; DMF, rt, 4h; **b)** TFA/water, rt, 4h.

anthraquinones available as commercial product. Then, the amino derivative (**10**) was obtained from a catalytic reduction of the nitro group, as reported in Scheme **1**. Compound **11** was obtained from aloe emodin (**16**) and the Boc-Ile-OSu derivative. The Boc protecting group was removed using a standard procedure, as reported in Scheme **2**. Compound **12** was obtained from juglone **17** and resorcinol, as shown in Scheme **3**. The structure of the product was confirmed by NMR. Compound **13** was obtained by nucleophilic substitution of bromine in a previously obtained compound **18** with potassium phthalimide (Gabriel synthesis, Scheme **4**) [29]. Finally, the synthesis of 5,9-di-hydroxybenzo[b]naphtho[2.1-d]furan (**14**) was accomplished by means of a literature procedure [30] used for the preparation of **19** (Scheme **5**). The two products were separated and (**14**) was characterized too.

Melting points were determined in capillary tubes and are uncorrected. Nuclear magnetic resonance (NMR) spectra were recorded on a Bruker Avance AMX 300 spectrometer and 1H NMR spectra were run using $CDCl_3$, CD_3OD, $(CD_3)_2CO$ or $(CD_3)_2SO$ as solvent and the solvent peak was used as internal standard. Chemical shifts (δ) are expressed in parts per million relative to tetramethylsilane (ppm), and spin multiplicities are indicated as an s (singlet), br s (broad singlet), d (doublet), dd (double doublet), t (triplet), and m (multiplet) and the values expressed in Hz. Analytical thin-layer chromatography (TLC) was carried out on precoated silica gel plates (Merck 60F254), and spots were visualized with a UV light at 254 nm. Column chromatography was performed using Merck silica gel (230-400 mesh). All starting materials not described below, the solvents, and the deuterated solvents were purchased from commercial sources, mainly Aldrich and Fluka. All reagents and solvents were used as received from commercial sources without additional purification, unless differently stated. Elemental analysis (CHN) was within 0.4% of the calculated values and was performed on a Carlo Erba 1016 elemental analyser. High resolution mass spectra (HRMS) were obtained using a MarinerTM API-TOF (Perceptive Biosystems Inc.-Framingham MA 01701 USA).

4,5-dihydroxy-1-nitroanthraquinone (15) [28]

KNO_3 (3.2 g, 0.032 mol) was added to a solution of 1,8-dihydroxyanthraquinone (5.0 g, 0.021 mol) in glacial acetic acid (400 ml). The reaction mixture was heated to 50°C for 15 minutes, then cooled and stirred at room temperature for 12 hours. Water (250 ml) was added to the mixture and the resulting precipitate was filtered out and purified by column chromatography on silica gel (toluene/cyclohexane = 1:1). The residue after evaporation of the solvent was again purified by column chromatography (toluene/ethyl acetate = 9:1) to give the pure title compound (2.0 g, 33% yield). mp 244°C; ^1H, $(CD_3)_2SO$: δ 12.38 (br s, 1H), 11.69 (br s, 1H), 8.07 (d, J = 9.0 Hz, 1H), 7.82 (dd, J = 9.0 Hz, J = 8.0 Hz, 1H), 7.63 (d, J = 9.0 Hz, 1H), 7.51 (d, J = 9.0 Hz, 1H), 7.41 (d, J = 8.0 Hz, 1H); HRMS calculated for $C_{14}H_8NO_6$ [M

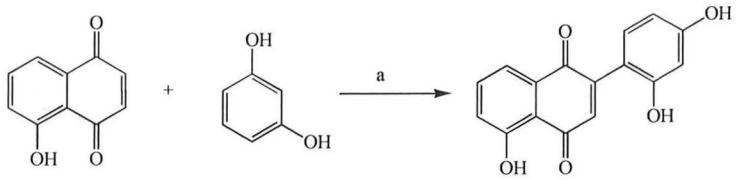

17 12

Scheme 3. a) H_3PO_4, CH_3COOH, rt, 2h under argon atmosphere.

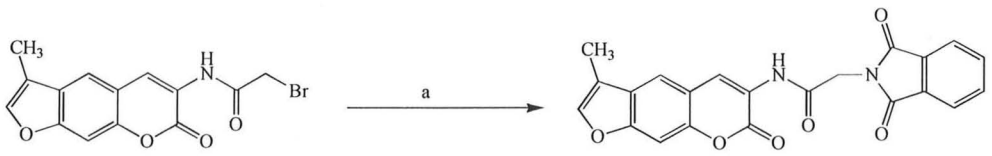

18 13

Scheme 4. a) Potassium phthalimide, DMA, rt, 4h.

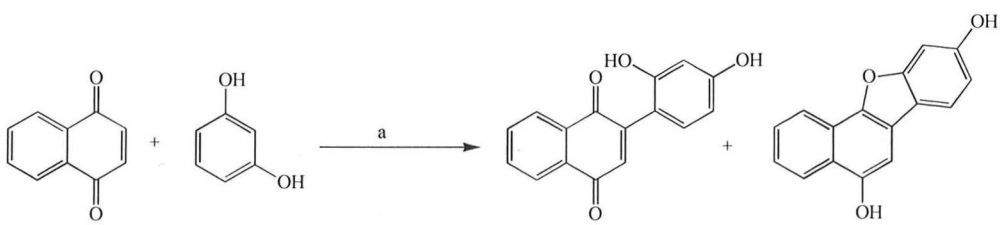

19 14

Scheme 5. a) H_2SO_4, CH_3COOH, rt, 2h.

+H]$^+$ 286.2150, found 286.1627. Elemental analysis (%) calculated for $C_{14}H_7NO_6$: C 58.96, H 2.47, N 4.91; found C 59.11, H 2.48, N 4.90.

1-amino-4,5-dihydroxyanthraquinone (10)

Pd/C (9 mg) was added to a solution of 1-nitro-4,5-dihydroxyanthraquinone (1.0 g, 3.5 mmol) in methanol (25 ml). The reaction mixture was stirred at room temperature under hydrogen. After 4 hours the catalyst was filtered out and the resulting solution was concentrated to dryness under reduced pressure to afford the title compound (878 mg, 98% yield). mp 269-271 °C; ^{1}H, $(CD_3)_2SO$: δ 12.81 (br s, 1H), 12,20 (br s, 1H), 8.42 (br s, 2H), 7.80 (q, *J* = 7.7 Hz, *J* = 7.6 Hz, 1H), 7.76 (dd, *J* = 7.6 Hz, *J* = 1.7 Hz, 1H), 7.38 (d, *J* = 9.4 Hz, 1H), 7.28 (dd, *J* = 7.7 Hz, *J* = 1.7 Hz, 1H), 7.27 (d, *J* = 9.4 Hz, 1H); HRMS calculated for $C_{14}H_{10}NO_4$ [M +H]$^+$ 256.0604, found 256.0421. Elemental analysis (%) calculated for $C_{14}H_9NO_4$: C 65.88, H 3.55, N 5.49; found C 65.91, H 3.54, N 5.51.

L-Isoleucine, (9,10-dihydro-4,5-dihydroxy-9,10-dioxo-2-anthracenyl)methyl ester (11)

Triethylamine (0.2 ml, 1.48 mmol), Boc-Ile-OSu (486 mg, 1.48 mmol) and dimethylaminopyridine (18 mg, 0.148 mmol) were added to a solution of aloe emodin (**16**) (200 mg, 0.74 mmol) in dimethylformamide (20 ml),. The reaction mixture was stirred at room temperature for 4 hours, and then water was added. The precipitate was filtered and the crude product was purified by column chromatography on silica gel. TFA 90% was added to the yellow solid obtained and the solution was stirred for 1 hour at rt, the trifluoroacetate salt was precipitated adding diethyl ether (1,5 ml) to the reaction mixture at 0°C. The title product was isolated as yellow solid (112 mg, yield 40%). Mp 187-189 °C; ^{1}H, CD_3OD: δ11.88 (br s, 2H), 7.81 (dd, *J* = 7.4 Hz, *J* = 1.7 Hz, 1H), 7.79 (d, *J* = 2.1 Hz, 1H), 7.78 (dd, *J* = 7.5 Hz, *J* = 7.4 Hz, 1H), 7.36 (dd, *J* = 7.5 Hz, *J* = 1.7 Hz, 1H), 7.34 (d, *J* = 2.1 Hz, 1H), 5.41 (s, 2H), 4.15 (d, *J* = 4.0 Hz, 1H), 2.15-1.95 (m, 1H), 1.60-1.30 (m, 2H), 1.06 (d, *J* = 7.0 Hz, 3H), 1.01 (t, *J* = 7.4 Hz, 3H); HRMS calculated for $C_{21}H_{22}NO_6$ [M +H]$^+$ 384.1308, found 384.1442. Elemental analysis (%) calculated for $C_{21}H_{22}NO_6$. $C_2F_3O_2$: C 55.54, H 4.46, N 2.82; found C 55.53, H 4,47, N 2.82.

5-hydroxy-2-(2,4-dihydroxyphenyl)-1,4-naphthoquinone (12)

A solution of resorcine (76 mg, 0.69 mmol) in acetic acid (2 ml), and then 0.5 ml of phosphoric acid was added to a solution of 5-hydroxy-1,4-naphtoquinone (17) (200 mg, 1.15 mmol) in acetic acid (10 ml). The reaction mixture was stirred at room temperature for 2 hours under argon atmosphere.

After that the mixture was diluted with water, and then neutralized with 5% sodium bicarbonate, and then extracted with ethyl acetate (3 × 15 ml).

The combined extracts were dried over sodium sulfate and evaporated to dryness. Purification of the residue by column chromatography on silica gel (eluent: hexane/ethyl acetate = 7:3 v/v), gave 200 mg of a solid (yield: 62%): mp 201-204 °C; ^{1}H $(CD_3)_2CO$: δ 11.99 (s,1H), 8.54 (br s, 2H), 7.63 (dd, *J* = 8.3 Hz, *J* = 7.2 Hz, 1H), 7.46 (d, *J* = 7.2 Hz, 1H), 7.18 (d, *J* = 8.3 Hz, 1H), 7.07 (d, *J* = 8.4 Hz, 1H), 6.89 (s, 1H), 6.39 (d, *J* = 2.1 Hz, 1H), 6.34 (dd, *J* = 8.4 Hz, *J* = 2.1 Hz, 1H); HRMS calculated for $C_{16}H_9O_5$ [M + H]$^-$ 281.2501; found 281.2551. Elemental analysis (%) calculated for $C_{16}H_{10}O_5$: C 68.09, H 3.57; found C 67.96, H 3.58.

Synthesis of 3-(ω-phthalimido-acetamido)-4'-methylpsoralene (13) [29]

0.2 g (0.6 mmol) of 3-(ω-bromoacetamido)-4'-methylpsoralen (18) and a solution of 0.14 g (0.76 mmol) of potassium phthalimide in 10.20 ml (109 mmol) of N,N-dimethylacetamide was stirred at room temperature for 4 hours (TLC: dichloromethane/ethyl acetate = 96:4 v/v). Then, 0.5 ml of glacial acetic acid was added and the mixture was stirred overnight.

The following morning a precipitate of a white solid was found in the solution. This was filtrated and washed with ethylic ether, and then dried to gave 201 mg of a pure white solid (yield: 83%): mp 312 °C; ^{1}H $CDCl_3$: δ 8.77 (s, 1H), 8.65 (s, 1H), 7.95-7.92 (m, 2H), 7.80-7.73 (m, 2H), 7.52 (s, 1H), 7.46 (d, J = 1.4Hz, 1H), 7.43 (d, J = 1.4Hz, 1H), 4.58 (s, 2H), 2.25 (s, 3H); HRMS calculated for $C_{22}H_{15}N_2O_6$ [M + H]$^{++}$ 403.0925; found 403.0991. Elemental analysis (%) calculated for $C_{22}H_{14}N_2O_6$: C 65.67, H 3.51, N 6.96; found C 65.65, H 3.52, N 6.99.

Synthesis of 5,9-di-hydroxybenzo[b]naphtho[2.1-d]furan (14) and of 2-(2,4-Dihydroxyphenyl)-1,4-naphthoquinone (19) [30].

A solution of resorcinol (139 mg, 1.26 mmol) in acetic acid (5 ml) was added to a solution of 1,4-naphthoquinone (400 mg, 2.53 mmol) in acetic acid (15 ml). Then, 2M sulphuric acid (1 ml) was added and the mixture was stirred at room temperature for 2 hours.

After that the mixture was diluted with water, and then neutralized with 5% sodium bicarbonate. and extracted with ethyl acetate (3 × 15 ml). The combined extracts were dried over sodium sulfate and evaporated to dryness. Compounds (**19**) and (**14**) were separated by column chromatography on silica gel (eluent: hexane/ethyl acetate = 6:4 v/v) and the separated spots were (**19**) (120 mg, 36%) and (**14**) (6 mg, 2%).

^{1}H (**14**) $(CD_3)_2CO$: δ 8.36 (d, J = 8.3Hz, 1H), 8.26 (d, J = 8.3Hz, 1H), 7.81 (d, J=8.6Hz, 1H), 7.67-7.63 (m, 1H), 7.56-7.50 (m, 1H), 7.41 (s, 1H), 7.16 (d, J = 1.7Hz, 1H), 6.93 (dd, J = 8.6Hz and J = 1.7Hz, 1H), 2.25 (s, 3H); HRMS calculated for $C_{16}H_{11}O_3$ [M + H]$^+$ 251,2563; found 251,2651. Elemental analysis (%) calculated for $C_{16}H_{10}O_3$: C 76.79, H 4.03; found C 76.76, H 4.02.

^{1}H (**19**) $(CD_3)_2SO$: δ 9.68 (br s, 2H), 8.03-7.96 (m, 2H), 7.88-7.82 (m, 2H), 7.05 (d, J = 8.4Hz, 1H), 7.00 (s, 1H), 6.38 (d, J = 2.2Hz, 1H), 6.30 (dd, J = 8.4Hz and J = 2.2Hz, 1H); HRMS calculated for $C_{16}H_{11}O_4$ [M + H]$^+$ 267,2678; found 267,0651. Elemental analysis (%) calculated for $C_{16}H_{10}O_4$: C 72.18, H 3.79; found C 72.15, H 3.82.

PKA Activity Assay

PKA activity was routinely assayed in the presence of 50 mM Tris-HCl pH 7.5, 12 mM $MgCl_2$, 0.02 mM [^{33}P-ATP] (500-1000 cpm/pmol), 1 μM cAMP, and using

Table 2. Docking Validation: Root Mean Square Deviation (RMSD, Å) of the Coordinates of the Best Scoring Docked Pose Relative to the Crystallographic Pose (Only Heavy Atoms have been Considered)

#	GOLD	Glide	eHiTS	MOE	PLANTS
1	5.58	8.17	7.98	6.69	2.07
2	0.93	0.50	10.53	3.10	0.59
3	7.08	1.50	2.25	2.89	0.88
4	2.13	0.33	3.07	2.21	2.67
5	0.83	1.12	3.81	2.34	0.97
6	2.66	5.03	5.31	3.12	5.96
7	3.18	0.78	4.21	3.23	1.48
8	1.02	2.80	1.35	2.52	2.67
9	2.29	1.65	3.02	3.11	1.53

ALRRASLGAA as synthetic peptide substrate, either in the absence or in the presence of increasing concentrations of inhibitors. Inhibition data for a range of concentrations of each competitive inhibitor at a constant concentration of the nucleotide phosphate donor were plotted against inhibitor concentrations to give the IC_{50} value.

RESULTS AND DISCUSSION

Protein Structure Selection

The nine protein structures were superposed and visual inspected carefully. With the only exception of 1SZM and 1STC structures, the rotamers of the active site residue side chains are conserved. Among the seven conserved structures, we selected the one with the best resolution (PDB code: 1Q8U). In particular, the sequence of 1Q8U is referred to a bovine PKA and it was compared to the human isoform (Swiss Prot access number P17612), resulting in a 98% residue identity. Moreover, all the residues of the catalytic pocket are conserved between the two sequences. The structure was therefore used in the docking experiments without further modifications.

Docking Phase Optimization

Due to the relative independence of the docking and scoring processes in virtual screening, we decided to optimize each step separately. The choice of the docking performance criteria depends on the amount and on the quality of information available on the protein target. In our case, the choice was rather straightforward, since the availability in the Protein Data Bank of several crystallographic structures complexed with different inhibitors. We assessed the ability of different docking approaches to reproduce the experimentally observed ligand conformations.

An ideal docking strategy for the virtual screening of medium to large sized databases has to be fast and able to retrieve the correct pose of a certain molecule as the top-scored predicted structure.

Table **2** shows the root mean square deviation (RMSD) between the heavy atom ligand coordinates of the best docked structure compared with the crystal structure. We chose 2.0 Å as a threshold for the RMSD value, considering a docking successful if the resulting RMSD was lower than 2.0 Å. Glide was identified as the best performing algorithm in this experiment, with six successes. Plants showed a comparable performance, with 5 successes and one result very close to the threshold (2.07). They were therefore, both selected to generate poses for the database molecules to be used in the scoring function optimization process.

Scoring Phase Optimization

The database was constructed to contain the structures of the 9 co-crystallized inhibitors (Fig. **2**), resulting in a final size of 467 molecules. These structures were docked with both the best-performing docking protocols, and the resulting poses were scored with the 11 scoring functions described earlier. For each docking-scoring combination receiver operating characteristic (ROC) and enrichment curves were generated, to assess its performance.

Table **3** summarizes the values of the integral of ROC curves for each docking-scoring pair. The integral value corresponds to the probability of an active molecule being scored better than a random molecule from the database.

As expected, the three consensus scoring schemes showed an overall good performance in combination with Fit10 generally performing best. Moreover, this performance was confirmed by the application of the protocol to other molecular databases, while the occasional better performance of some of the single functions appears to be highly database-dependent (data not shown).

Fig. (**3**) shows the enrichment curves for the three consensus functions applied with both docking procedures. Despite the lower ROC integral values, PLANTS shows a better enrichment profile, with a maximum enrichment factor in the top 10% of 6.7 (5.6 for GLIDE). The top 10% lists of both docking programs with the Fit10 consensus rescoring were visual inspected for the final hit selection. Five candidates were selected on the basis of the best topological and chemical complementarity with the ATP-binding cleft and covering the highest chemical diversity among the other high ranking molecules.

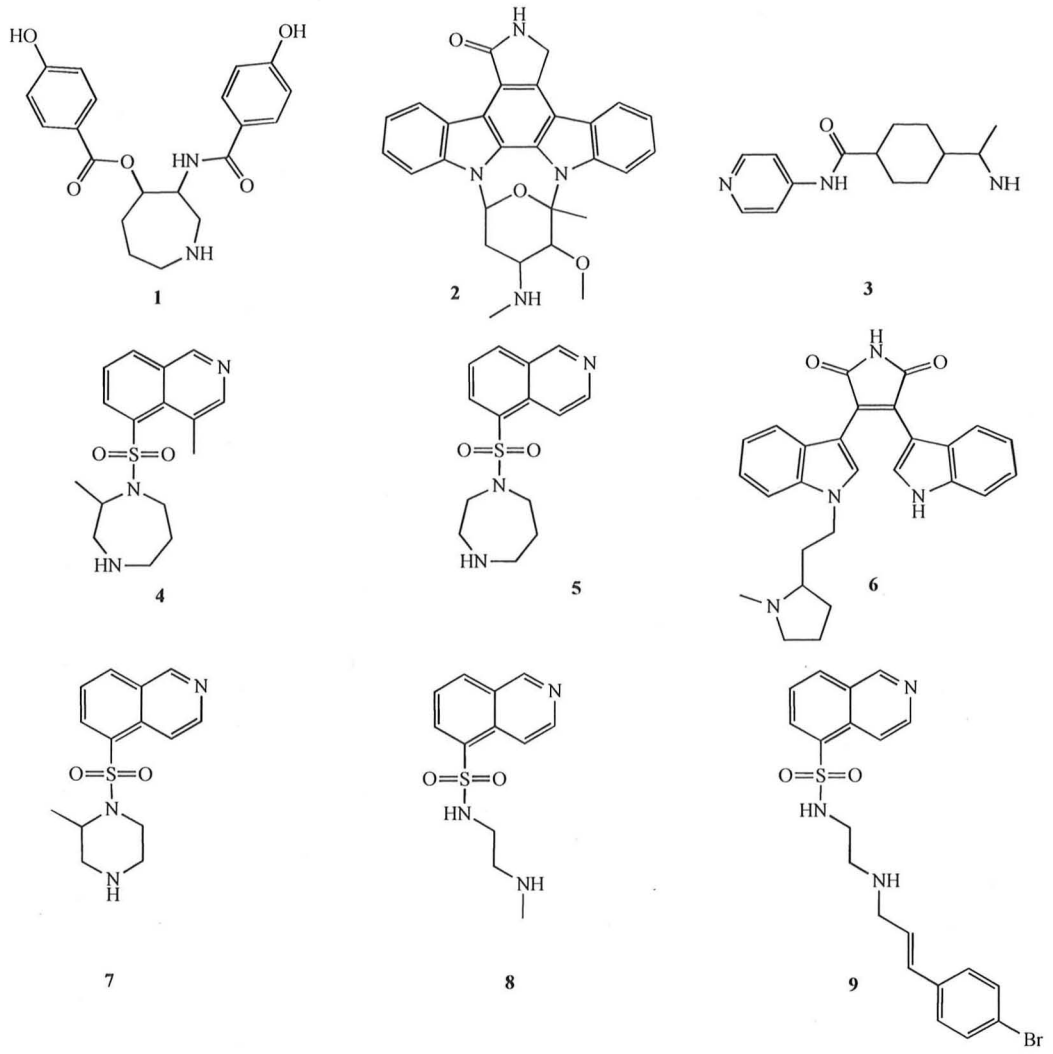

Fig. (2). PKA inhibitors used in the docking validation step.

Table 3. Scoring Validation: Integrals Values for the ROC Curves Relative to each Scoring Function on the Test Database (Probability of the Scoring Function Giving a Better Score to a known Active Compound than to a Random One)

Scoring Function	Glide	Plants
Fit10	0.87	0.75
NCS	0.85	0.72
LCS	0.82	0.74
PLP	0.84	0.69
Chemgauss 2	0.81	0.73
MOEscore	0.80	0.58
Chemgauss	0.78	0.76
Screenscore	0.74	0.67
X-Score	0.72	0.59
Zapbind	0.71	0.50
Chemscore	0.65	0.61

Fig. (3). Enrichment curves for NCS (blue), LCS (yellow) and Fit10 (red) consensus functions. The top figure refers to poses generated with GLIDE, the bottom one to poses generated with PLANTS.

The five molecules were tested *in vitro* for their inhibitory activity against PKA and are displayed in Table **4**, where the IC_{50} values for their inhibition are also reported. It can be seen that the first four compounds do not inhibit PKA activity at concentrations below 40 μM. Interestingly, the anthraquinone derivative **11** displays an IC_{50} value around 27μM. A comparison between the compounds listed in Table **1** is showed in Fig. (**4**) where the dose-dependent curves of PKA inhibition are reported.

Table 4.

#	Inhibition $IC_{50}(\mu M)^a$
10	>60
11	27
12	50
13	47
14	45
19	>60

[a]The values of IC50 represent the means of at least three independent experiments with SEM never exceeding 15%.

Fig. (4). Dose dependent inhibition of protein kinase PKA. The activity of PKA was determined by incubation, as described in the experimental section.

In particular, according to our docking model, derivative 11 interacts with the hinge region of the kinase through three hydrogen bonds: firstly with the backbone carbonyl and nitrogen of Val123, secondly with the backbone carbonyl of Glu121 (Fig. **5**). On the other hand, the fused ring system is engaged in several hydrophobic interactions (Val57, Ala70, Val104, Val123, Leu173). The binding mode and the interaction network of the anthraquinone moiety is very close to the one observed for adenine in the binding of ATP. Additionally, the alpha amine of the isoleucine tail forms a salt bridge with the side chain of Glu91 and the sec-butyl is in close proximity with hydrophobic residues such as Phe54 and Val57.

Finally, we have also tested these new PKA inhibitors against a very small panel of other kinases, such as protein kinase CK2, the protein kinase CK1δ, and GSK3β, and all of them shown an IC_{50} values higher than 100 μM. Further investigations are carrying out in our laboratories to better describe their selectivity profiles and to improve their binding affinities against PKA.

CONCLUSION

Computational methods such as ligand-docking have nowadays become almost routine techniques in medicinal chemistry, and are widely used in both the lead-discovery and the lead-optimization phases in rational drug design. An accurate estimation of the docking free energy remains the most difficult task. To speed up the calculation of the free energy, most docking programs implement approximated scoring functions of various kinds. Nevertheless, it has been widely shown that such scoring functions have a limited reliability. A possible solution is to use the consensus-scoring approach and we have reported an encouraging application of this strategy in discovering a novel class of protein kinase A inhibitors. Further investigations are in progress in our laboratories to extend and verify the applicability of this approach against other therapeutically interesting drug targets.

ACKNOWLEDGEMENT

The molecular modeling work coordinated by S.M. has been carried out with financial supports of the Italian Minis-

Fig. (5). Binding mode of derivative **11**. *on the left*: prediction of the stabilizing interaction network. Hydrogen-bonds (blue arrows) and charge-charge interactions (green arrows) are shown. Solvent exposed areas are marked by a blue halo. *on the right*: the PLANTS best predicted binding pose of derivative **11** inside PKA active site.

try for University and Research (MIUR), Rome, Italy and of the University of Padova, Padova, Italy. S.M. is also very grateful to Chemical Computing Group for the scientific and technical partnership.

REFERENCES

[1] Seifert, M. H.; Lang, M. Essential factors for successful virtual screening. *Mini Rev. Med. Chem.*, **2008**, *8*, 63-72.

[2] Lyne, P. D. Structure-based virtual screening. an overview. *Drug Discov., Today*, **2002**, *7*, 1047-1055.

[3] Doman, T. N.; McGovern, S. L.; Witherbee, B. J.; Kasten, T. P.; Kurumbail, R; Stallings, W. C.; Connolly, D. T.; Schoichet, B. K. Molecular docking and high-throughput screening for novel inhibitors of protein tyrosine phophatase-1B. *J. Med. Chem.*, **2002**, *45*, 2213-2221.

[4] Majeux, N.; Scarsi, M.; Apostolakis, J.; Caisch, A. Exhaustive docking of molecular fragments on protein binding sites with electrostatic solvation. *Proteins*, **1999**, *37*, 88-105.

[5] Kellenberger, E.; Rodrigo, J.; Muller, P.; Rognan, D. Comparative evaluation of eight docking tools for docking and virtual screening accuracy. *Proteins*, **2004**, *57*, 225-242.

[6] Muegge, I.; Martin, Y. C. A general and fast scoring function for protein-ligand interactions. A simplified potential approach. *J. Med. Chem.*, **1999**, *42*, 791-804.

[7] Bortolato, A.; Moro, S. Designing a ligand for pharmaceutical purposes. *Expert Opin. Drug Descov.*, **2008**, *3*, 579-590.

[8] Cozza, G.; Bonvini, P.; Zorzi, E.; Poletto, G.; Pagano, M.A.; Sarno, S.; Donella-Deana, A.; Zagotto, G.; Rosolen, A.; Pinna, L.A.; Meggio, F.; Moro, S. Identification of ellagic acid as potent inhibitor of protein kinase CK2: a successful example of a virtual screening application. *J. Med. Chem.*, **2006**, *49*, 2363-2366.

[9] Moro, S.; Bacilieri, M.; Deflorian, F. Combining ligand-based and structure-based design in the virtual screening arena. *Expert Opin. Drug Descov.*, **2007**, *2*, 37-49.

[10] Chiaradonna, F.; Balestrier,i C.; Gaglio, D.; Vanoni, M. RAS and PKA pathways in cancer: new insight from transcriptional analysis. *Front Biosci.*, **2008**, *13*, 5257-5278.

[11] Masciocchi, J.; Frau, G.; Fanton, M.; Sturlese, M.; Floris, M.; Pireddu, L.; Palla, P.; Cedrati, F.; Rodriguez-Tomé, P.; Moro, S. MMsINC: a large-scale chemoinformatics database. *Nucleic Acids Res.* **2009**, *37*, D284-290; http.//mms.dsfarm.unipd.it/MMsINC.html

[12] Berman, H.M.; Westbrook, J.; Feng, Z.; Gilliland, G.; Bhat, T.N.; Weissig, H.; Shindyalov, I.N.; Bourne, P.E. The protein data bank. *Nucleic Acids Res.*, **2000**, *8*, 235-242.

[13] Molecular Operating Environment (MOE 2004.03), C. C. G., Inc, 1255 University St., Suite 1600, Montreal, Quebec, Canada, H3B 3X3; http.//www.chemcomp.com

[14] LigPrep, version 2.1, Schrödinger, LLC, New York, NY, **2005**.

[15] Charifson, P.S.; Corkery, J.J.; Murcko, M.A; Walters, W.P. Consensus scoring. a method for obtaining improved hit rates from docking databases of three-dimensional structures into proteins *J. Med. Chem.*, **1999**, *42*, 5100-5109.

[16] Chen, J.Z.; Wang, J.;Xie, X.Q. GPCR structure-based virtual screening approach for CB2 antagonist search. *J. Chem. Inf. Model*, **2007**, *47*, 1626-1637.

[17] Schultz-Gasch, T.M. Stahl binding site characteristics in structure-based virtual screening. evaluation of current docking tools. *J. Mol. Model*, **2003**, *9*, 47-57.

[18] Eldridge, M.D.; Murray, C.W.; Auton, T.R.; Paolini, G.V.; Mee, R.P.; Empirical scoring functions. I. The development of a fast empirical scoring function to estimate the binding affinity of ligands in receptor complexes. *J. Comput.-Aided Mol. Des. (JCAMD)*, **1997**, *11*, 425-445.

[19] Stahl, M.; Rarey, M. Detailed analysis of scoring functions for virtual screening. *J. Med. Chem.*, **2001**, *44*, 1035-1042.

[20] Wang, R.; Lai, L.; Wang, S. Further development and validation of empirical scoring functions for structure-based binding affinity prediction. *J. Comput.-Aided Mol. Des.*, **2002**, *16*, 11-26.

[21] Verkivker, G.M.; Bouzida, D.; Gehlaar, D.K.; Rejto, P.A.; Arthurs, S.; Colson, A.B.; Freer, S.T.; Larson, V.; Luty, B.A.; Marrone, T.;Rose, P.W. Deciphering common failures in molecular docking of ligand-protein complexes. *J. Comput.-Aided Mol. Des. (JCAMD)*, **2000**, *14*, 731-751.

[22] Verdonk, M. L.; Cole, J.C.; Hartshorn, M. J.; Murray, C.W.; Taylor, R.D. Improved protein-ligand docking using GOLD. *Proteins*, **2003**, *52*, 609-623.

[23] Korb, O.; Stützle, T.; Exner, T.E. PLANTS: Application of Ant Colony Optimization to Structure-Based Drug Design. In: Dorigo, M.; Gambardella, L.M.; Birattari, M.; Martinoli, A.; Poli, R.; Stützle, T. (Eds.) Ant Colony Optimization and Swarm Intelligence, 5th International Workshop, ANTS **2006**, LNCS *4150*, 247-258.

[24] Korb, O.; Stützle, T.; Exner, T. E. An ant colony optimization approach to flexible protein-ligand docking. *Swarm Intell.*, **2007**, *1*, 115-134.

[25] Korb, O.; Stützle, T.; Exner, T. E. Empirical scoring functions for advanced protein-ligand docking with PLANTS. *J. Chem. Inf. Model*, **2009**, *49*, 84-96.

[26] Halgren, T.A.; Myrphy, R.B; Friesner, R.A.; Beard, H.S.; Frye, L.L.; Pollard, W.T. Glide: a new approach for rapid, accurate docking and scoring 1 methods and assessment of docking accuracy. *J. Med. Chem.*, **2004**, *47*, 1739-1749.

[27] Zsoldos, Z.; Reid, D.; Simon, A.; Sadjad, S.B.; Johnson, A.P. eHiTS. a new fast, exhaustive flexible ligand docking system. *J. Mol. Graph. Model.*, **2007** *26*, 198-212.

[28] Antonello, C.; Uriarte, E.; Palumbo, M. Diethylaminopropionamido-hydroxy-anthraquinones as potential anticancer agents. synthesis and characterization. *Archiv. Der. Pharmazie*, **1989**, *322*, 541-544.

[29] Santana, L.; Uriarte, E.; Gonzlez-Daz, H.; Zagotto, G.; Soto-Otero, R.; Mndez-Ivarez, E. A QSAR model for in silico screening of MAO-A inhibitors. Prediction, synthesis and biological assay of novel coumarins. *J. Med. Chem.*, **2006**, *49*, 1149-1156.

[30] Hogberg, H.E. Cyclo-oligomerization of Quinone. *Acta Chem. Scand.*, **1973**, *27*, 2559-2566.